

XPS Study of Aged Polyaniline Films

V. Jousseume, M. Morsli, A. Bonnet

Laboratoire de Physique des Solides pour l'Electronique, Université de Nantes, 2 rue de la Houssinière, BP 92208, 44322 Nantes cedex 03, France

Received 3 June 2002; accepted 4 May 2003

ABSTRACT: In this article, a study of the aging of conducting Polyaniline–Polystyrene blends using X-ray photoelectron spectroscopy (XPS) and UV-visible-near IR analysis is presented. The physicochemical results are compared to those obtained by electrical measurements. XPS results confirm the existence of an oxidation process also deduced by the electrical conductivity studies. The N1s and S2p core level spectra decomposition allows to show that a deprotonation process and cyclization of tertiary amine occur during aging. The absorption spectrum shows a decrease of

delocalized charges and the apparition of localized polarons after a long aging time. All these mechanisms are responsible of the electrical conductivity decrease observed during aging at elevated temperature. The results are presented for films of PANI–CSA–PSt blends, but the conclusions can be extended to pure conducting PANI–CSA films. © 2003 Wiley Periodicals, Inc. *J Appl Polym Sci* 90: 3730–3736, 2003

Key words: conducting polymers; polyaniline

INTRODUCTION

Polyaniline (PANI) is always one of the most promising conducting polymers. It can be used in many electronic applications such as organic light emitting diodes, batteries, and for electromagnetic shielding.^{1–4} Blends of PANI with an insulating polymer (polystyrene, cellulose acetate, etc.) are also interesting for these applications because these composites associate the electrical properties of polyaniline and the mechanical properties of the host polymer.^{5–7} But for each application, the stability of PANI is crucial and a good comprehension of the degradation mechanisms is necessary. At our knowledge, also few works are devoted to the study of the thermal and time stability of PANI and PANI blends.^{8–12}

The purpose of this work is to correlate electrical measurements and physicochemical analysis (XPS, UV-Vis absorption) of aged films. Previous studies have shown that electrical measurements in PANI can be interpreted in the frame of an heterogeneous model where the conduction is limited by hopping mechanisms between conducting clusters separated by insulating or less doped regions. The same heterogeneous model can also be applied in PANI blends.¹³ In this case, a very low percolation threshold has been obtained (less than 1%). Above this percolation threshold, an interpenetrating fibrillar network of PANI exists, which cross over all the host material and the electrical conductivity is mainly limited by hopping mecha-

nisms between conducting clusters among each PANI fibril. The artificial aging at high temperature of polyaniline films and polyaniline–polystyrene (PANI–PSt) blends have been previously studied by electrical measurements and the results have been interpreted in the frame of the heterogeneous electrical model.¹³ The aging observed has been related to an increase of the intercluster region to the detriment of the conducting clusters. But electrical measurements fail to associate the erosion of the conducting clusters in polyaniline films with physical or chemical processes such as oxygen reaction with the backbone, deprotonation, dopant decomposition or segregation, crosslinking.

In this article, an interpretation of the artificial aging at elevated temperature of PANI–PSt blends is proposed using XPS and electrical measurements. The evolution of the C1s, O1s, N1s, and S2p elements with the aging time and the decomposition of the N1s and S2p peaks are shown. The physicochemical results are compared with electrical measurements, and the different mechanisms at the origin of the irreversible decrease of the electrical conductivity are proposed.

EXPERIMENTAL

Undoped polyaniline have been synthesized by using the standard procedure.¹⁴ High conductive PANI–CSA films (where CSA is camphor sulfonic acid) have been prepared by casting a PANI–CSA *m*-cresol solution on a hot glass substrate ($\sigma = 250$ S/cm). Conducting polyaniline–polystyrene blends (PANI–PSt) have been prepared as described previously, using the co-dissolution method.¹³ Depending on the PANI content in the blend, the electrical conductivity at room tem-

Correspondence to: M. Morsli

perature varies between 10^{-11} S/cm for 0.3% of PANI in the blend to 70 S/cm for 5% of PANI in the polystyrene matrix. In this type of blends, the percolation threshold is very low ($<1\%$), this behavior being related to the formation of a self-assembled interpenetrating fibrillar network of PANI in the host matrix.⁷ In the text, blends above the percolation threshold are referred to as conducting blends. Different pieces of the same films have been artificially aged in a thermostat oven at 130°C at room atmosphere. The electrical conductivity has been continuously monitored *in situ* using a two contacts method (by using a Keithley 2000). Samples have been collected after different aging times, and electrical conductivity measurements vs. temperature and physicochemical analysis have been carried out. Electrical conductivity measurements vs. temperature have been performed in the temperature range of 80–300 K following the standard four contacts method using a Keithley 220 current source and a Keithley 182 voltmeter. X-Ray Photoelectron Spectroscopy (XPS) measurements have been carried out with a Leybold LHS 12 apparatus (University of Nantes–CNRS) using magnesium as the source of radiation (1253.6 eV) at 10 kV and 10 mA. The pass energy was set at 50 eV. The vacuum in the analysis chamber was about 10^{-6} Pa. High resolutions scans with a good signal ratio have been obtained in the C1s, N1s, O1s, and S2p regions of the spectrum. The quantitative analysis has been based on the determination of the C1s, N1s, O1s, and S2p peak areas with 0.2, 0.36, 0.61, and 0.44 as sensitivity factors. All the spectra have been recorded under identical conditions. The decomposition of the XPS peaks into different components and the quantitative interpretation have been performed after subtraction of the background using the Shirley method.¹⁵ The curve-fitting programs allow the variation of parameters such as the Gaussian-Lorentzian ratio, the full width at half maximum (FWHM), the position, and the intensity of each contribution. These parameters have been optimized by the curve-fitting program. UV-Vis absorption spectra have been recorded using a Varian Cary 2400 Spectrophotometer.

RESULTS AND DISCUSSION

PANI films and PANI-PSt blends are electrically stable materials at room temperature, and they do not present a significant decrease of the electrical conductivity for more than 3 years. At more elevated temperature (between 80 and 150°C), a decrease of the electrical conductivity is observed with a similar aging kinetic in PANI and in PANI-PSt blends above the percolation threshold. Previous works have also shown that the aging rate increases with the aging temperature.¹⁰ Figure 1 shows typical electrical conductivity variations vs. time for a PANI–CSA–PSt 3% film aged at 130°C .

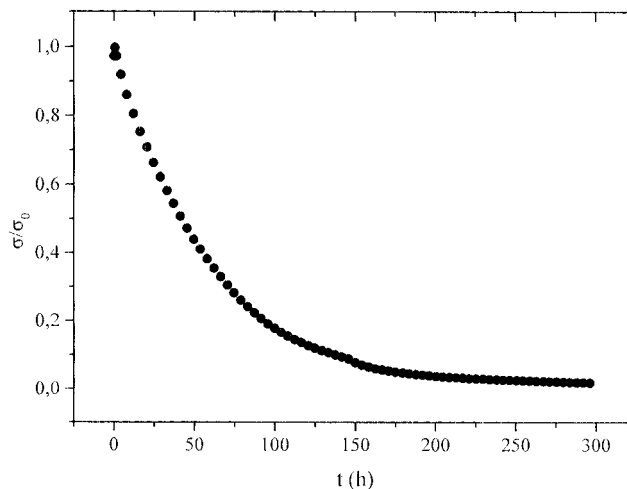


Figure 1 Variations of σ/σ_0 vs. time for a PANI–CSA–PSt 3% film aged at 130°C .

film that has been aged at a temperature of 130°C for more than 1 month. This sample is a blend above the percolation threshold. This graph reveals that the electrical conductivity decreases with time from 0.3 S/cm for a fresh sample to 3×10^{-4} S/cm after 1245 h of aging at 130°C . A simple Arrhenius law (sometimes observed in some conducting polymers^{12,16,17}) fails to describe these experimental variations in the whole time range studied. As for PANI–CSA and other PANI–CSA–PSt blends, two aging time domains should be distinguished. A $(\sigma_0 - \sigma)/\sigma_0 = At^{1/2}$ law allows to describe the first part of the curve (for short aging time) up to $\sigma = \sigma_0/2$. This kind of law has been previously discussed,¹⁸ and indicates that oxygen diffusion into the film is the slowest process in the degradation mechanism. For long aging time, an exponential law $\sigma = \sigma_1 \exp[-(t/\tau)^2]$ can be used to fit experimental results. This complex kinetic law also observed in other conducting polymers¹⁹ is difficult to link to the reaction of oxygen on the polymer backbone or to other processes liable to interact in the aging process (deprotonation, change of structure, etc.). To specify the evolution of the conduction mechanisms with the aging time, electrical conductivity measurements vs. temperature can be useful. In Figure 2, the electrical conductivity as a function of the temperature is shown for different aging times for PANI–PSt 3% films. The results obtained are in accordance with a previous study already published on the same type of blends.¹⁰ At low temperature, the electrical conductivity is thermally activated, and the slope of the curve increases with the aging time. These experimental results can be interpreted in the frame of an heterogeneous picture. In this case, the electrical conductivity at low temperature is dominated by an hopping mechanism between conducting clusters of PANI through a very thin insulating or less doped/

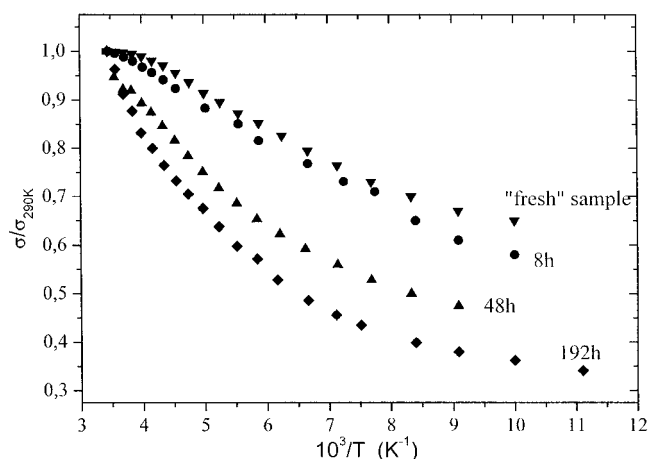


Figure 2 Variations of σ/σ_{290} vs. $1000/T$ for PANI-CSA-PSt 7% blends after aging at 130°C for different durations.

ordered barrier. For a fresh sample, the result can be interpreted using the Fluctuation Induced Tunneling model.²⁰

$$\left(\text{FIT}, \sigma \propto \exp \left[- \left(\frac{T_0}{T_1 + T} \right) \right] \right)$$

The FIT model can also be applied for short aging sample (up to $\sigma = \sigma_0/2$). For long aging time, a transition from the FIT model toward the Charging Energy Limiting Tunneling model is observed.²¹

$$\left(\text{CELT}, \sigma \propto \exp \left[- \left(\frac{T_0}{T} \right)^{1/2} \right] \right)$$

This transition from the FIT model to the CELT model has been first discussed by Sheng,²⁰ and it depends essentially of the cluster size and the intercluster width. In this granular model, the increase of the $\sigma(T)$ curve slope is directly related with the increase of the grain size (see ref. 22 for the complete theory and grain size formula). Then, the main conclusion of this electrical study is that because the slope of the $\sigma(T)$ curve increases with the aging time, the grain size of the conducting clusters decreases, and the intercluster width increases with the aging time. Moreover, the change of transport mechanisms (FIT toward CELT), also observed in polypyrrole films,¹⁹ seems to be consistent with the crossover of the short thermal conductivity decay following a parabolic law toward a non-trivial stretched exponential behavior.

The UV-Visible-near IR absorption of PANI-CSA has been extensively described in the literature^{23–25} and the absorption spectra of PANI-CSA-PSt blends and pure PANI-CSA films are similar even for low concentration of PANI in the blend. Figure 3 shows the variations of the absorption spectra of PANI-CSA-

PSt samples aged for different durations. The “fresh” sample shows an absorption spectra in accordance with those of pure PANI-CSA. The first peak at 440 nm can be attributed to the transition between polaronic band and the π^* band. As in pure PANI-CSA, a large band extending to the near IR is observed which can be associated to the presence of delocalized defects (free carrier tail). These absorption spectra can also be linked to the conformation of the polyaniline.²³ In this case, the free carrier tail can be associated with delocalization of electrons in the polaron band promoted by a straightening-out of the polymer chain as its coil-like structures becomes more expanded with concomitant reduction in π defects caused by ring twisting.

During aging, the large band in the near IR decreases in intensity, which indicates that the expanded coil-like conformation are converted to the more coil-like conformation. As pointed by McDiarmid and Epstein,²³ this behavior should be accompanied by a decrease of the film crystallinity and should train a decrease of the electrical conductivity. After more than 1240 h of aging at 130°C , a large peak at 815 nm begins to appear in the absorption spectra. This peak is traditionally attributed to the presence of localized electrical defects. Then, the artificial aging seems to lead to an increase of the charge localization, may be due to the decrease of the film crystallinity and of the expanded coil-like conformation.

Figure 4 shows the evolution of C1s XPS spectrum with the aging time (between $t = 0$ (fresh sample) and $t = 1245$ h at 130°C). The C—C bond at 284.7 eV has been used as the reference peak, and some XPS spectrum have been corrected because for the more aged samples, a charging effect has been observed. Table I shows that the carbon concentration decreases with the aging time from 81.6% for a fresh sample to 73.7%

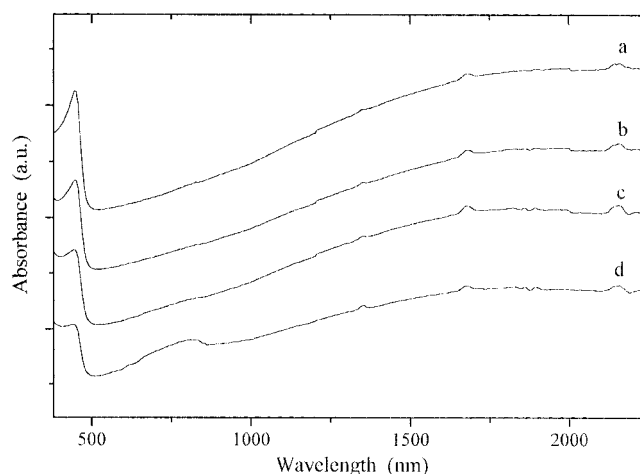


Figure 3 UV-visible-near IR spectra of PANI-CSA-PSt blends after aging at 130°C for different durations. (a) “fresh” sample; (b) 48 h; (c) 264 h; (d) 1245 h.

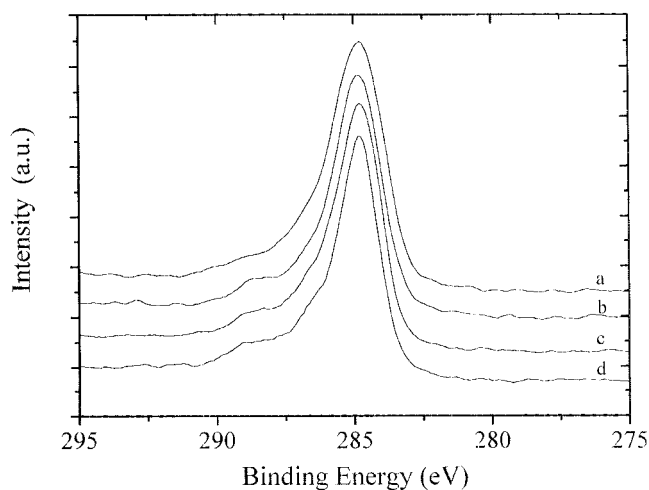


Figure 4 XPS C1s core level spectra of PANI-CSA-PSt 3% blends after different aging times at 130°C. (a) "fresh" sample; (b) 48 h; (c) 264 h; (d) 1245 h.

after 1245 h of aging at 130°C. The decomposition of the C1s spectra is not shown here because it involves lots of different bonds difficult to resolve. For example, the energy difference between the different carbon-oxygen bonds is too small to be resolved. However, some details can be seen studying the evolution of the shape of the C1s spectra.

The shape of the C1s spectra shows an increase of the contribution situated near 289 eV. This high binding energy can be attributed to the presence of carboxyl or ester groups.²⁶ These COOR groups, where the creation involves complex mechanisms, have also been observed during the aging of other conducting polymers composites^{27,28} for long aging time at room temperature. For short aging time, the same work shows that the oxidation occurs under the form of C=O bonds observed near 286.5 eV and C—O—H bonds observed between 286.5 and 287 eV.^{26,29} Such contributions can also be envisaged here. Then, the increase with the aging time of the high binding energy domain in the C1s spectra indicates a progressive oxidation of the film. In addition, it must be noticed that the C/N ratio, which can be calculated from Table I, results is higher than expected (theoretically 9): this additional carbon reveals a superficial contamination during atmosphere exposure.

TABLE I
Relative Surface Composition (%) of C1s, O1s, N1s, and S2p in PANI-CSA-PSt 3%

	C1s	O1s	N1s	S2p
Fresh samples	81.6	13.1	3.5	1.8
After 48 h at 130°C	77.4	18.6	2.9	1.1
After 264 h at 130°C	77.3	18.6	3.1	1.0
After 1245 h at 130°C	73.7	22.5	3.0	0.8

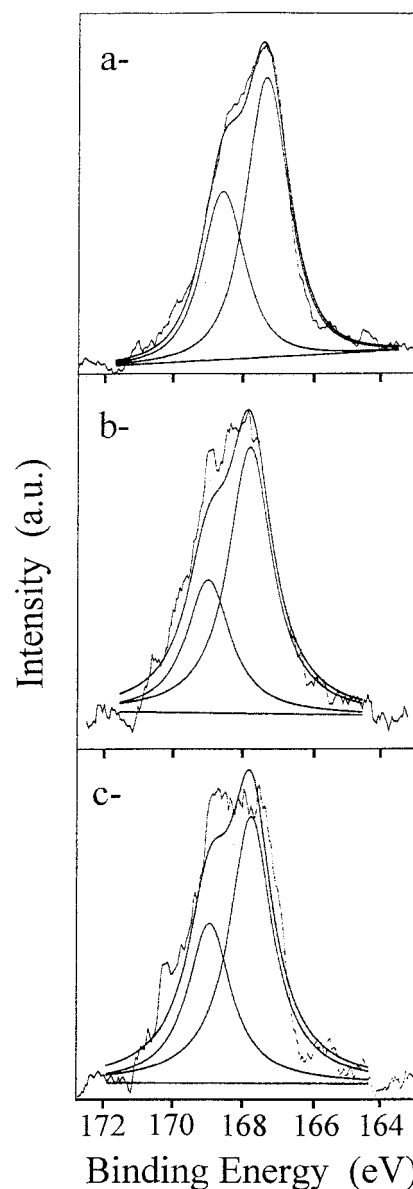


Figure 5 XPS S2p core level spectra of PANI-CSA-PSt 3% blends after different aging times at 130°C. (a) "fresh" sample; (b) 48 h; (c) 264 h.

Additional information concerning the oxidation process can be obtained by the observation of the O1s contribution. Table I shows that the oxygen percentage increases from 13.1% for a fresh sample to 22.5% after 1245h at 130°C, which confirms that oxidation is an important phenomenon that occurs during the aging process. Then, both C1s and O1s unequivocally show that oxidation occurs upon aging of PANI-PSt blends.

Figure 5 shows the S2p peak decomposition for different aging times. The S2p core level signal attributed to the covalently bonded sulfonate anion ($-\text{SO}_3^-$) can be fitted with the spin-orbit doublet S2p3/2 and S2p1/2 lying at about 167.3 eV and 168.6 eV, respectively.^{30,31} The absence of peak in the low binding

TABLE II
XPS Analysis of PANI-CSA-PSt 3% Blend during Aging

	N1s			S2p	
	N ₁	N ₂	N ₃	S2p3/2	S2p1/2
"Fresh" samples					
BE (eV)	399.24	400.55	401.99	167.3	168.58
Intensity (%)	50.8	29.4	19.8	50	50
After 48 h at 130°C					
BE (eV)	399.21	400.19	401.67	167.76	168.96
Intensity (%)	40.9	45.3	13.8	50	50
After 264 h at 130°C					
BE (eV)	399.37	400.37	401.70	167.76	168.96
Intensity (%)	44.3	49.3	6.4	50	50

energy domain (163.8 eV) due to neutral S species shows that all the S2p is used in the protonation process. Another contribution situated near 169.5 eV and attributed to the existence of sulfonate anions in PANI-CSA in a more electron rich condition³¹ is not present in our film.

The evolution of the decomposition of the S2p peak during aging does not show any drastic change, and the (—SO₃) contribution is also observed after 1245 h of aging at 130°C, with no significant change in the percentage of each peak (Table II). On the other hand, the decrease of the S2p percentage in the film from 1.8% for a fresh sample to 0.8% after 1245 h of aging at 130°C can be associated to a loss of dopant (CSA) upon aging. Figure 6 shows that the S/N ratio, which is near 0.53 for a fresh sample (theoretically 0.5), decreases with the aging time up to 0.27 after 1245 h of aging at 130°C. Then, the decrease of the S2p percentage can be related to a loss of CSA, leading to a deprotonation of the conducting film. Other works have also proposed that an aggregation of CSA can occur upon a thermal treatment of a PANI-CSA film.³² This process is also possible during the aging of our conducting blends.

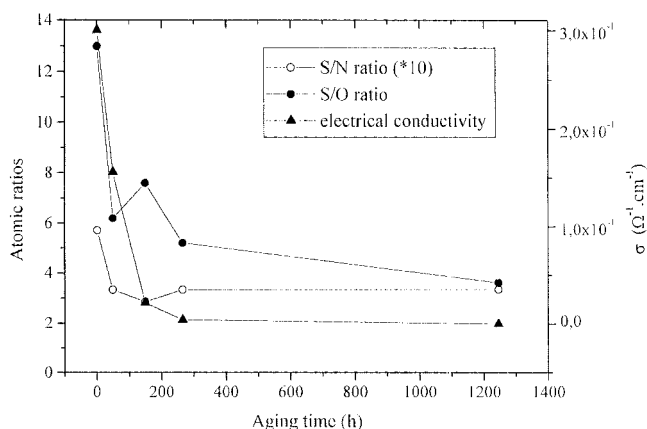


Figure 6 Atomic ratio (obtained by XPS measurements) and electrical conductivity of PANI-CSA-PSt films aged at 130°C vs. the aging time.

The XPS N1s core level spectrum of "fresh" PANI-CSA-PSt 3% film is shown in Figure 7. Three main contributions can be considered. The first peak situated at 399.2 eV can be attributed to amine nitrogen (—NH).^{33,34} Two other peaks separated by 1.3 eV and 2.8 eV, respectively, from the amine peak are com-

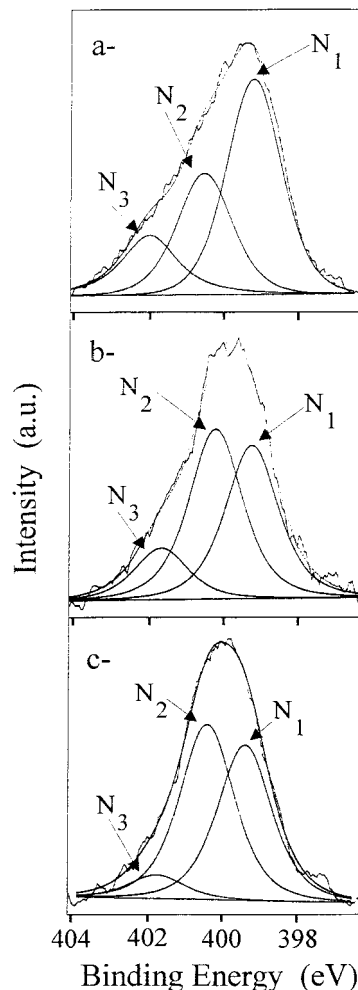


Figure 7 XPS N1s core level spectra of PANI-CSA-PSt 3% blends after different aging times at 130°C. (a) "fresh" sample; (b) 48 h; (c) 264 h.

monly assigned to N^+ species.^{31,33,34} In undoped polyaniline or in noncompletely protonated polyaniline, a peak present at 398 eV attributed to imine nitrogen ($-N=$) is also observed.³⁴ This contribution is not present in our PANI-PSt, samples which shows that all the imine nitrogen have been protonated. The N^+/N ratio is nearly to 0.5 for a fresh sample, which is consistent with the dopant content used during the protonation process (1/2 dopant molecule per repeat polymer unit involving one ring and one nitrogen). This decomposition is of the same type as in pure PANI-CSA.

Upon aging, the N1s percentage decreases from 3.5% for a fresh sample to 2.9% after 48 h of aging at 130°C. This percentage is then constant upon aging (near 3%) up to 1245 h of aging at 130°C. Figure 7 shows that the decomposition of the N1s peak of aged samples shows also three components as for "fresh" film. The first component near 399.2 eV, which is attributed to amine nitrogen decreases with the aging time from 50.8% at $t = 0$ to 44.3% after 264 h of aging at 130°C (Table II). In the same time, the N_2 peak near 400.5 eV increases from 29.4 to 49.3%, and the N_3 peak decreases from 19.8 to 6.4%. These two contributions habitually attributed to N^+ species should be discussed with precaution because XPS is not the best tool for elucidating the molecular structure. The deprotonation of the film pointed out by the study of the S2p contribution should be accompanied by a decrease of the N^+ species. The N_3 peak (N^+ species more localized) decreases with aging. But the increase of the N_2 peak with the aging time is difficult to explain if this peak is unequivocally attributed to N^+ species. However, the N_2 peak could also be attributed to cyclic nitrogen >N- (near 400 eV).^{35,36} As been pointed by Ranou et al.,⁸ the progressive deprotonation upon aging can entail crosslinking by formation of these tertiary amine nitrogen bonds on expense imine bonds.

Within all these results, a more accurate view of aging in conducting polyaniline blends can be obtained. The electrical measurements converge toward a heterogeneous picture of polyaniline, even in PANI-PSt blends. Conducting clusters in which PANI is well ordered and more crystallized and in which electrical defect are delocalized are separated by thin insulating nonordered or less doped region in which carriers are more localized. Upon aging, several physical and chemical mechanisms take place simultaneously. Oxygen diffusion occurs preferentially at the periphery of the conducting clusters leading to an erosion of the clusters. The diffusion of oxygen should be favored by the disorder of the intercluster region. XPS experiments show an increase of the high binding energy of the C1s peak, which can be associated with the formation of carbonyl COOH or COOR groups. An increase of the $C=O$ and $C-O-H$ contaminations cannot be excluded. Optical absorption shows a decrease of the IR tail (i.e., delocalized electrical defects associated

with a expended coil conformation). This decrease is consistent with a less extended coil conformation of the film, that is, an increase of the disordered region. For long aging time, a localized polaron contribution appears in the absorption spectra.

XPS measurements show that a loss of dopant is observed leading to a deprotonation of the film. This progressive deprotonation is accompanied by an increase of the N_2 contribution in the N1s peak that was previously attributed exclusively to N^+ species. To explain this last result, a cyclization of the tertiary amine nitrogen process should be introduced.

CONCLUSION

Electrical measurements and physicochemical analysis have been carried out on aged samples in the aim to specify the aging process in conducting PANI-CSA-PSt blends. The results are consistent with the heterogeneous picture previously proposed, where conducting clusters are separated by thin insulating barriers. The electrical conductivity decrease observed upon aging can be associated to an oxygen diffusion in the film. For long aging time, it has been more difficult to link the conductivity decrease with a simple oxygen diffusion or reaction in the film. Optical absorption measurements and XPS analysis confirm the oxidation of the film. These experiments also show a decrease of the dopant content, which can be associated to the dopant loss. This loss of dopant is followed by a deprotonation of the conducting film leading to the cyclization of the tertiary amine nitrogen and to a possible crosslinking of the polyaniline.

References

- de Lima, J. R.; Schreiner, C.; Hümmelgen, I. A.; Fornari, C. C. M., Jr.; Ferreira, C. A.; Nart, F. C. *J Appl Physics* 1998, 84, 1445.
- Halliday, D. P.; Eggleston, J. M.; Adams, P. N.; Pentland, I. A.; Monkman, A. P. *Synth Met* 1997, 85, 1245.
- Liess, M.; Chinn, D.; Petelenz, D.; Janata, J. *Thin Solid Films* 1996, 286, 252.
- Cottevieille, D.; Le Méhauté, A.; Challioui, C.; Mirebeau, P.; Demay, J. N. *Synth Met* 1999, 101, 703.
- Jousseau, V.; Morsli, M.; Bonnet, A.; Tesson, O.; Lefrant, S. *J Appl Polym Sci* 1998, 67, 1205.
- Pron, A.; Nicolau, Y.; Genoud, F.; Nechtschein, M. *J Appl Polym Sci* 1997, 63, 971.
- Reghu, M.; Yoon, C. O.; Yang, C. Y.; Moses, D.; Smith, P.; Heeger, A. J.; Cao, Y. *Phys Rev B* 1994, 50, 13931.
- Rannou, P.; Nicolau, Y. F.; Nechtschein, M.; Ermolieff, A.; Rouchon, D. *Synth Met* 1999, 101, 823.
- Dalas, E.; Sakkopoulos, S.; Vitoratos, E. *Synth Met* 2000, 114, 365.
- Jousseau, V.; Morsli, M.; Bonnet, A. *J Appl Physics* 2000, 88, 960.
- Chandranthi, N.; Careem, M. A. *Polym Bull* 2000, 44, 101.
- Amano, K.; Ishikawa, H.; Kobayashi, A.; Satoh, M.; Hasegawa, E. *Synth Met* 1994, 62, 229.
- Jousseau, V.; Bonnet, A.; Morsli, M.; Cattin, L. *Eur Phys J Appl Physics* 1999, 6, 7.

14. Macdiarmid, A. G.; Chiang, J. C.; Richter, A. F.; Somasiri, N. L.; Epstein, A. J. *Conducting Polymers*; Alcazer, L., Ed.; Reidel: Dordrecht, 1987, p. 105.
15. Shirley, D. A. *Phys Rev B* 1972, 5, 6219.
16. Samuelson, L. A.; Druy, M. A. *Macromolecules* 1986, 19, 824.
17. Kuhn, H. H.; Child, A. D.; Kimbrell, W. C. *Synth Met* 1995, 71, 2139.
18. Truong, V. T. *Synth Met* 1992, 52, 33.
19. Sixou, B.; Mermilliod, N.; Travers, J. P. *Phys Rev B* 1996, 53, 4509.
20. Sheng, P.; Sichel, E. K.; Gittleman, J. J. *Phys Rev Lett* 1978, 40, 1197.
21. Sheng, P.; Abeles, B.; Arie, Y. *Phys Rev Lett* 1973, 31, 44.
22. Zuppiroli, L.; Bussac, M. N.; Paschen, S.; Chauvet, O.; Forro, L. *Phys Rev B* 1994, 50, 5196.
23. MacDiarmid, A. G.; Epstein, A. J. *Synth Met* 1995, 69, 85.
24. Cochet, M.; Corraze, B.; Quillard, S.; Buisson, J. P.; Lefrant, S.; Louarn, G. *Synth Met* 1997, 84, 757.
25. Nicolau, Y. F.; Beadle, P. M.; Banka, E. *Synth Met* 1997, 84, 585.
26. Beamon, G.; Briggs, D. *High Resolution XPS of Organic Polymers*; Wiley: New York, 1992.
27. Samir, F.; Morsli, M.; Bernede, J. C.; Bonnet, A.; Lefrant, S. *J Appl Polym Sci* 1997, 66, 1839.
28. Benseddik, E.; Makhoulouki, M.; Bernede, J. C.; Lefrant, S.; Pron, A. *Synth Met* 1995, 72, 237.
29. Burkstrand, J. M. *J Appl Physics* 1981, 52, 4795.
30. Neoh, K. G.; Kang, E. T.; Tan, K. L. *Polym Degrad Stabil* 1994, 43, 141.
31. Han, M. G.; Im, S. S. *Polymer* 2000, 41, 3253.
32. Yang, C. Y.; Reghu, M.; Heeger, A. J.; Cao, Y. *Synth Met* 1996, 79, 27.
33. Tan, K. L.; Tan, B. T.; Kang, E. T.; Neoh, K. G. *Phys Rev B* 1989, 39, 8079.
34. Jousseume, V.; Morsli, M.; Bonnet, A.; Lefrant, S. *J Appl Polym Sci* 1998, 67, 1209.
35. Rodrigue, D.; Riga, J.; Verbist, J. J.; *J Chim Phys* 1992, 89, 1209.
36. Demaret, X.; Cristallo, G.; Snauwaert, P.; Riga, J.; Verbist, J. J. *Synth Met* 1993, 55-57, 1051.